

# Field Weakening in Buried Permanent Magnet AC Motor Drives

BRIGETTE SNEYERS, DONALD W. NOVOTNY, SENIOR MEMBER, IEEE, AND THOMAS A. LIPO, SENIOR MEMBER, IEEE

**Abstract**—The usual uncoupled  $d - q$  model of salient pole synchronous machines (Park's model) may be insufficient for accurate modeling of buried magnet permanent magnet machines. The addition of a nonbilateral coupling between the direct and quadrature axis equivalent circuits is shown to improve the steady-state model greatly. The cross coupling reactance has important implications in improving operation in the constant horsepower mode. In particular, it is demonstrated that the cross coupling term acts to reduce the effective internal voltage so that some field weakening can be achieved. The results should be useful in permanent magnet machine design for variable speed drive applications.

## INTRODUCTION

**I**NDUCTION and synchronous motor static drives are presently in an advanced stage of development. In contrast, permanent magnetic motor drives have only recently begun active development. A primary motivating factor for this development is the interest in high-performance high-efficiency servomotor drives particularly for the machine tool industry. One of the primary limiting features of permanent magnet motor drives is the lack of excitation control. As a result, the internal EMF of the motor rises in proportion to the motor speed. Such behavior is desirable in the so-called constant torque range, since it is consistent with the constant volts per hertz control which is normally used during this mode of operation. However, when the speed continues to rise, the voltage limit of the associated frequency converter is reached. The motor is then said to enter the field weakening or constant horsepower model of operation. The internal voltage must now be adjusted to be compatible with the applied converter voltage. However, since the permanent magnets inherently provide the equivalent of a constant field excitation, the internal EMF of the machine continues to increase as speed increases. As a result, the motor power factor becomes leading and the current to be commutated by the inverter continues to increase as speed increases. In the case of a permanent magnet machine fed by a current source inverter, voltage stresses on the converter semiconductors also continue to rise, since the commutation spike increases with both motor internal voltage and dc link current.

It has recently been reported [1] that the expected performance in the high-speed region is not always observed. In the

case of machines of the so-called "buried magnet" type, the variations of the current and power factor are much smaller than expected on the basis of the conventional two-axis synchronous machine theory. The speed range above base speed for constant power operation is larger than the anticipated speed range before the torque decreases excessively. These special features are analyzed in this paper.

## NEW MODEL FOR BURIED PERMANENT MAGNET MOTORS

Recently, it has been suggested that the usual uncoupled  $d - q$  model of salient pole synchronous machines (Park's model) may be insufficient for accurate modeling of buried magnet permanent magnet machines [1]. In particular, if the conventional model is used, the direct axis synchronous reactance  $X_d$  varies in an erratic manner. For certain values of load, the value of  $X_d$  must even be negative if the equivalent circuit is expected to predict the observed values of direct and quadrature axes current. The presence of permanent magnets in the motor prevents use of most of the conventional parameter measurement methods. A simple way to approach the problem is to measure and identify the curves,  $V_d = f(I_q)$  and  $V_q = f(I_d)$ . The results for the  $q$  axis are shown in Fig. 1 for fixed speed. Since the equation of the equivalent circuit of the  $q$  axis is  $V_q = E + X_d I_d$ , all curves should cross at the same point for  $I_d = 0$ . The particular curve pattern of Fig. 1 seems to be a characteristic of buried permanent magnet machines [1]. It was observed that the distance between two curves for  $I_d = 0$  is proportional to  $I_q$ . The addition of a coupling term between the direct and quadrature axis is an obvious remedy, and the mathematical model of the permanent magnet machine is then rewritten as

$$\begin{aligned} V_d &= X_q I_q \\ V_q &= E + X_d I_d + X_{qd} I_q. \end{aligned}$$

If  $P$  is the number of poles and  $\omega$  is the operating frequency used to define the  $d - q$  reactances, then the torque equation becomes

$$\begin{aligned} T = \frac{3P}{4\omega} & \left[ \frac{VE}{X_d} \sin \delta \right. \\ & \left. + \frac{V^2(X_d - X_q)}{2X_d X_q} \sin 2\delta + \frac{V^2 X_{qd}}{X_d X_q} \sin^2 \delta \right]. \end{aligned}$$

The first two terms can readily be recognized as the magnet torque term and the reluctance torque term. The third term represents the contribution of the cross coupling, which

Paper IPCSD 84-11, approved by the Industrial Drives Committee of the IEEE Industrial Applications Society for presentation at the 1983 Industrial Applications Society, Annual Meeting, Mexico City, Mexico, October 3-7, 1983. Manuscript released for publication May 3, 1984. This work was supported by the Belgian American Educational Foundation.

B. Sneyers is with dienst ETEC, Vrije Universiteit Brussel, Pleinlaan 2, B-1050 Brussels, Belgium.

D. W. Novotny and T. A. Lipo are with the Department of Electrical and Computer Engineering, University of Wisconsin-Madison, 1415 Johnson Drive, Madison, WI 53706.

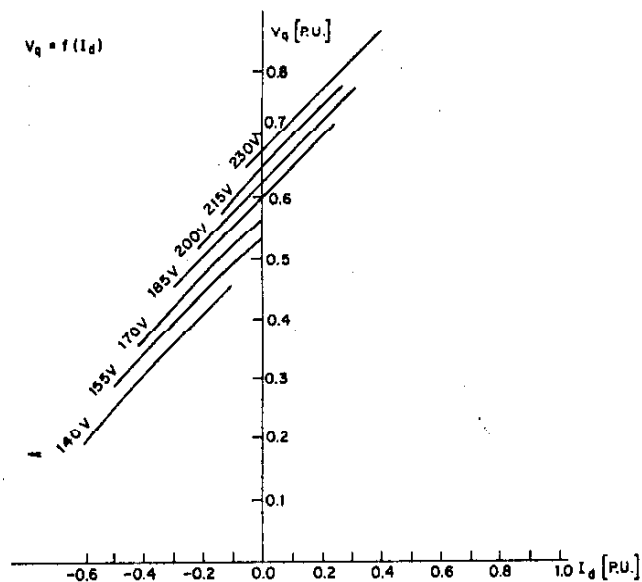


Fig. 1.  $q$  axis measurements:  $V_q = f(I_d)$ .

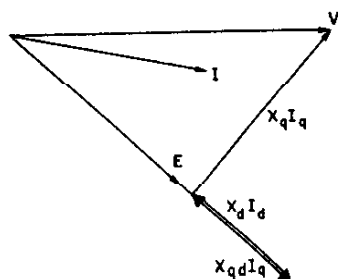


Fig. 2. Phasor diagram for new model.

depends on  $\sin^2 \delta$  and reaches a maximum for the same value of  $\delta$  as the magnet torque term.

The phasor diagram including the cross coupling term is shown in Fig. 2. Notice that the additional term modifies the internal voltage with respect to  $I_q$  in the same manner as a change in field current. In the case of buried magnet machines, the path for the  $q$  axis flux usually presents a lower reluctance than the  $d$  axis path where the magnets placed in the  $d$  axis have nearly the same reluctance as air. Consequently, the value of the reactance  $X_q$  will be larger than the value of the reactance  $X_d$ . The reluctance torque term will be negative, and the no-load operating point may occur at a value of  $\delta$  different than  $\delta = 0$ .

Using the new model and the measured values of  $V_q$ ,  $V_d$ ,  $I_q$ , and  $I_d$ , values of  $X_d$ ,  $X_q$ , and  $X_{qd}$  can be calculated. The results of such measurements are shown in Fig. 3. The continuous line shows the values of  $X_d$  needed to represent the characteristics of the machine with the classical  $d - q$  model. The crosses show the computed values of  $X_d$  using the new model. There is almost no variation for these new values, which is consistent with the fact that the magnets form most of the flux path in the  $d$  axis. However, saturation can be observed in the  $q$  axis as shown in Fig. 4. The cross coupling reactance  $X_{qd}$  was observed to have almost no dependence on  $I_q$  or  $I_d$ . There is, however, some dependence on flux levels as will be explained later.

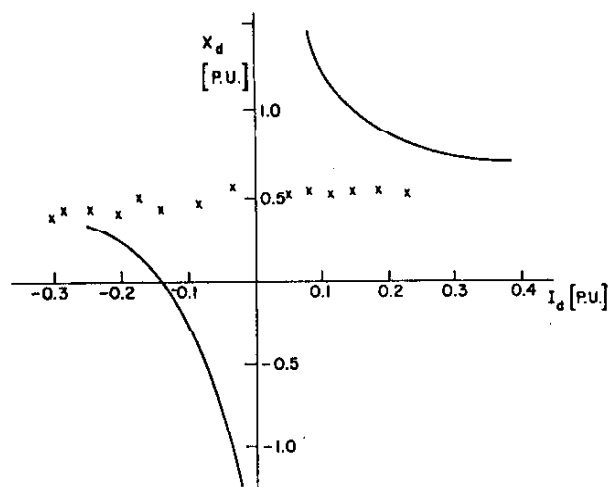


Fig. 3. Measured values for  $X_d$ . Solid lines are for conventional model, crosses are for new model.

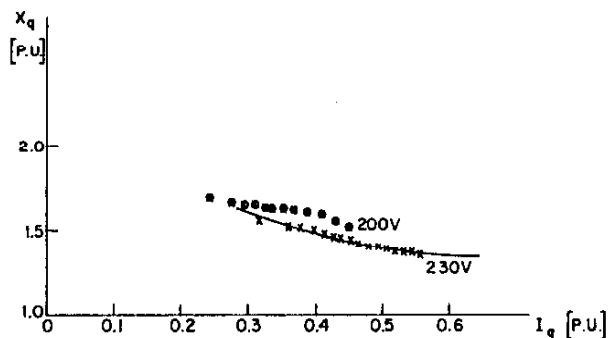


Fig. 4. Measured values of  $X_q$ .

### General Characteristics of the Machine

When considering the characteristics of a drive, two main operating speed ranges are distinguished—the constant torque region below base speed and the constant horsepower region above base speed. Figs. 5–8 illustrate the influence of the additional term in both cases for a simple machine without saliency. Above base speed, the voltage is usually kept constant at its rate value, limited by the rating of the converter. The current is limited by the rating of the machine. However, for the sake of comparison with dc machines, this mode of operation is often considered as a constant power region or field weakening region.

### Operation Above Base Speed

For constant power operation, Fig. 5 shows a comparison between two permanent magnet machines—one incorporating the cross coupling effect and one without the effect. Parameters are chosen so that, at base speed and rated torque, both machines have identical characteristics. The two conditions in Fig. 5 represent operation at speeds of 1.0 pu and 2.0 pu.  $E_1$  is the inner voltage for the conventional machine model for 1.0-pu speed.  $E_1'$  is the inner voltage for the machine with a cross coupling term. The difference is produced by the cross coupling term.

At 2.0 pu speed,  $E_1$  is doubled to  $E_2$ . The voltage and power

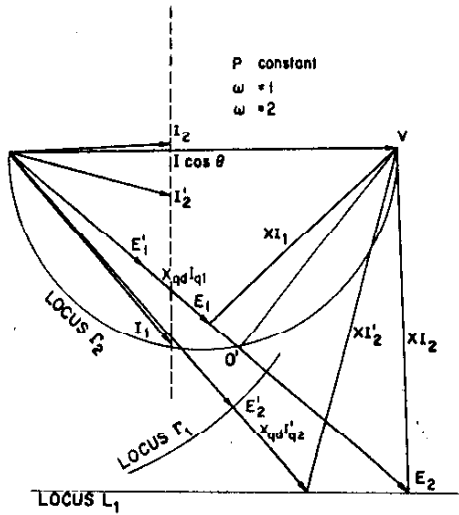


Fig. 5. Operation above base speed.  $P = \text{constant}$ .

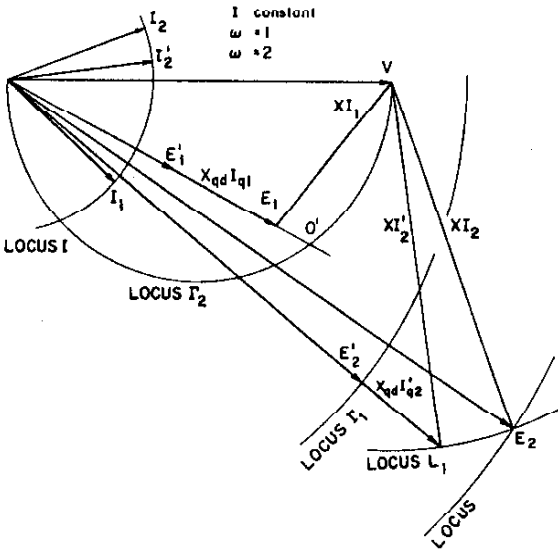


Fig. 6. Operation above base speed.  $I = \text{constant}$ .

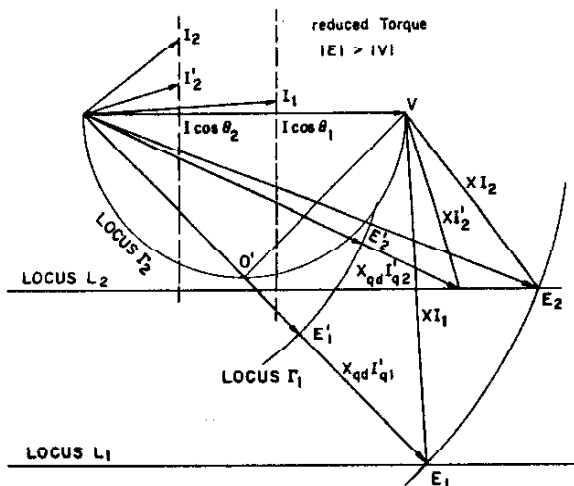


Fig. 7. Operation below base speed, overexcited operation.

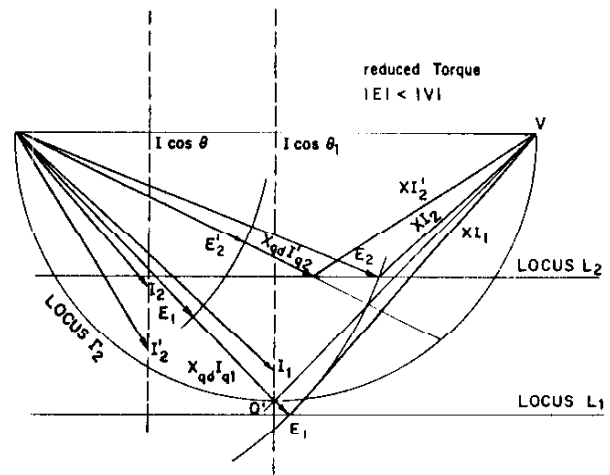


Fig. 8. Operation below base speed, underexcited operation.

are kept constant, so that  $I \cos \theta$  and  $XI \cos \theta$  are also constant. This last value gives the locus  $L_1$ , the locus of the inner voltage of the machine for 2.0-pu speed. From  $E_2$  and  $V$ , the vector  $XI_2$  is deduced and also the vector  $I_2$  which is the current of the machine without cross coupling effect at 2.0-pu speed. The solution of the machine with the cross coupling term is established as follows: the distance  $VO'$  is equal to  $XI_q$ , the distance  $E_1'E_1$  is equal to  $X_{qd}I_q$ . The ratio of these two distances will be a constant depending on the machine. Notice that for every load condition, the point  $O'$  will be on the circle  $\Gamma_2$ . The locus  $\Gamma_1$  is the locus of the inner voltage at 2.0-pu speed (caused by the magnets). The difference between  $\Gamma_1$  and  $L_1$  will be provided by the cross coupling term.

The ratio defined earlier allows us to find the solution presented in Fig. 5, which locates  $XI_2'$  and finally  $I_2'$ , the current of the machine with cross coupling effect at 2.0-pu speed. The solution  $I_2'$  lags the solution  $I_2$ , and this will always be the case. Depending on the respective values of  $E$ ,  $V$ , and of the parameters and operating point,  $I_2'$  will be larger or smaller than  $I_2$ . If speed increases, both currents will become leading, and  $I_2'$  will be smaller than  $I_2$ .

A similar case is shown in Fig. 6, but in this case, the voltage and current are kept constant. The same construction leads to the solution for  $I_2$  (machine without cross coupling) and  $I_2'$  (machine with cross coupling). The only differences are due to the fact that in this case the current is kept constant (locus  $L$ ) so that locus  $L_1$  becomes a circle centered at  $V$  ( $|XI|$  constant). The phasor diagram shows both machines with leading power factor. The power delivered by the machine with cross coupling will be, in this case, larger.

The influence of cross coupling in the speed range above base speed can easily be understood by considering the power equation. For smooth air gap machines  $P = EI_q$  is, in this case, the complete power expression. With rising speed, the counterelectromotive force (CEMF)  $E$  rises. The power  $P$  is kept constant which means that  $I_q$  decreases proportionally. Since the inner voltage of the machine with cross coupling is partly due to the magnets and partly proportional to  $I_q$ , it will not rise as much as if it were entirely due to the magnets. The effect will be field weakening, just as if the field had been modified.

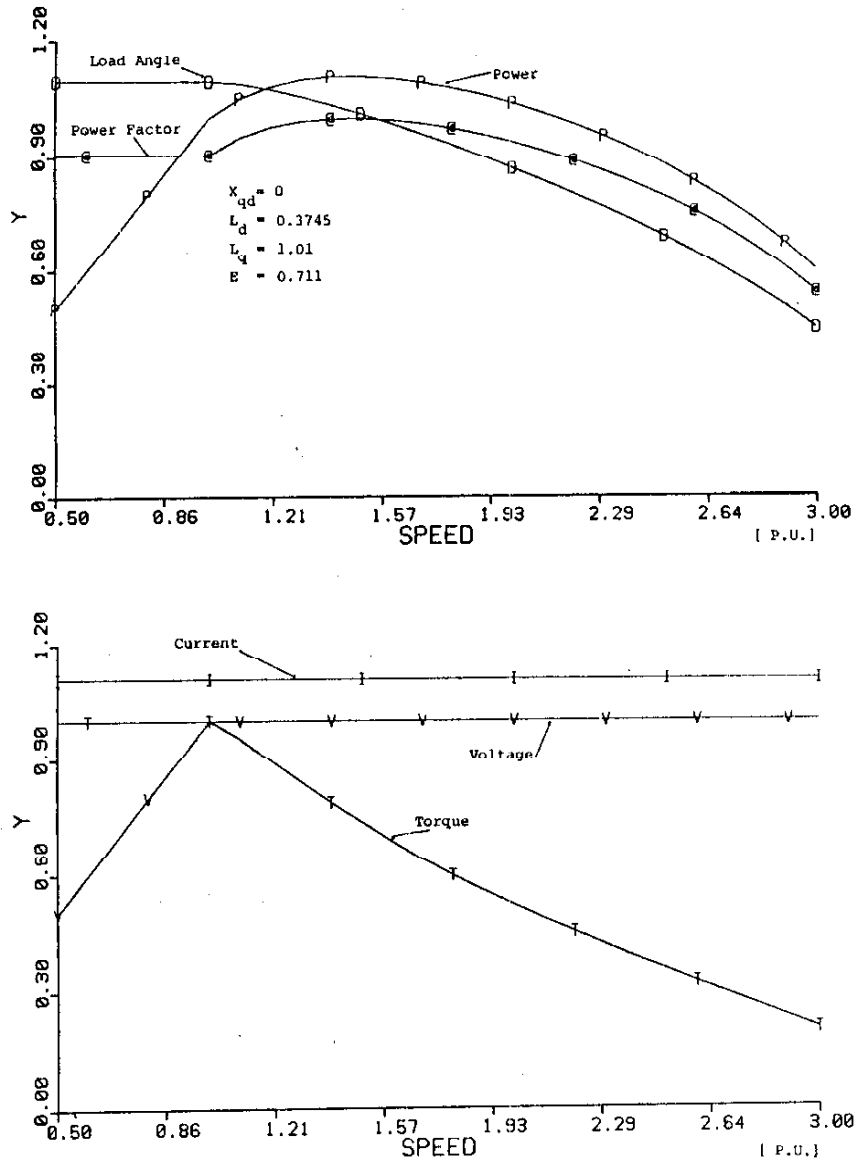


Fig. 9. Salient pole machine characteristics as function of speed. Machine without cross coupling, constant current operation.

**Operation Below Base Speed**

If the speed is kept constant and the torque reduced, the effect of the cross coupling will depend on the relative values of  $V$  and  $E$ . Fig. 7 shows the behavior at half-rated torque for the same two machines as in the previous section in the case of overexcited operation,  $|E| > |V|$ . Locus  $L_2$  is the locus of  $E$  for reduced torque where  $IX \cos \theta$  is reduced by a factor of two. The currents in this case will be leading, and the cross coupling will have an advantageous effect. Fig. 8 shows the same characteristics but for the case of two underexcited machines in which  $|E| < |V|$ . In this case, the current  $I_2'$ , lagging the current  $I_2$ , will be larger.

These factors can also be explained by the power equation  $P = EI_q$ . For a fixed speed,  $E$  remains constant, and as the torque and hence the power is reduced,  $I_q$  is reduced. As a consequence, the total inner voltage of the machine with cross coupling will be reduced, and  $I_q$  will be larger than for the machine without cross coupling.  $I'$  will lag  $I$  and, depending

on parameters and operating conditions, can be larger or smaller in amplitude than for a machine without cross coupling.

The phasor diagrams clearly show that for a smooth air gap machine, the current  $I'$  of a machine with cross coupling will always lag the current  $I$  of a machine without cross coupling with advantageous consequences above base speed and some disadvantages below base speed.

**Performance Curves—Advantages of Cross Coupling**

In general, machines have different reactances in the  $d$  and  $q$  axes. The diagrams and equations become more complex, and computer calculation becomes a necessity. Figs. 9–12 show salient pole machine characteristics as a function of the speed. In Fig. 9, the current is kept constant and the machine has no cross coupling. Fig. 10 shows the same characteristics for a machine with cross coupling. These curves have been calculated using the measured parameters of a 2-hp buried permanent magnet machine (Appendix). It is important to

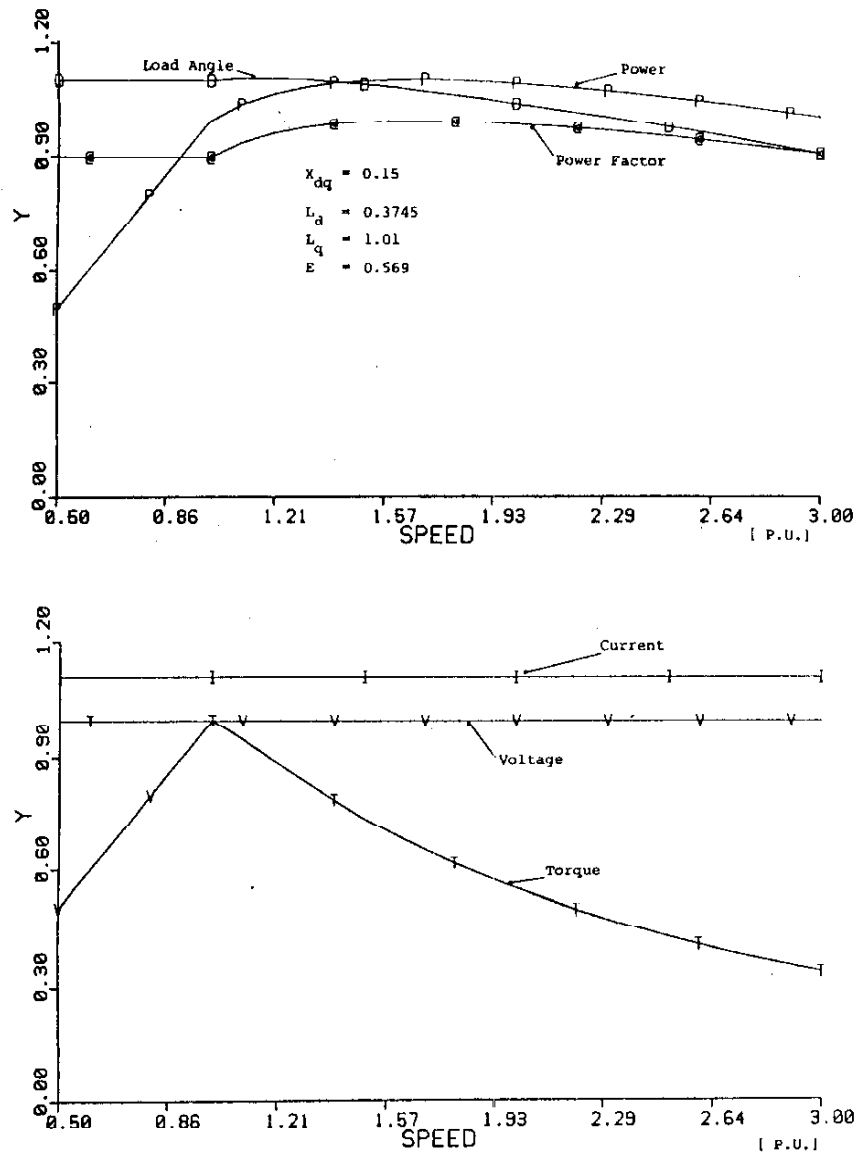


Fig. 10. Salient pole machine characteristics as function of speed. Machine with cross coupling, constant current operation.

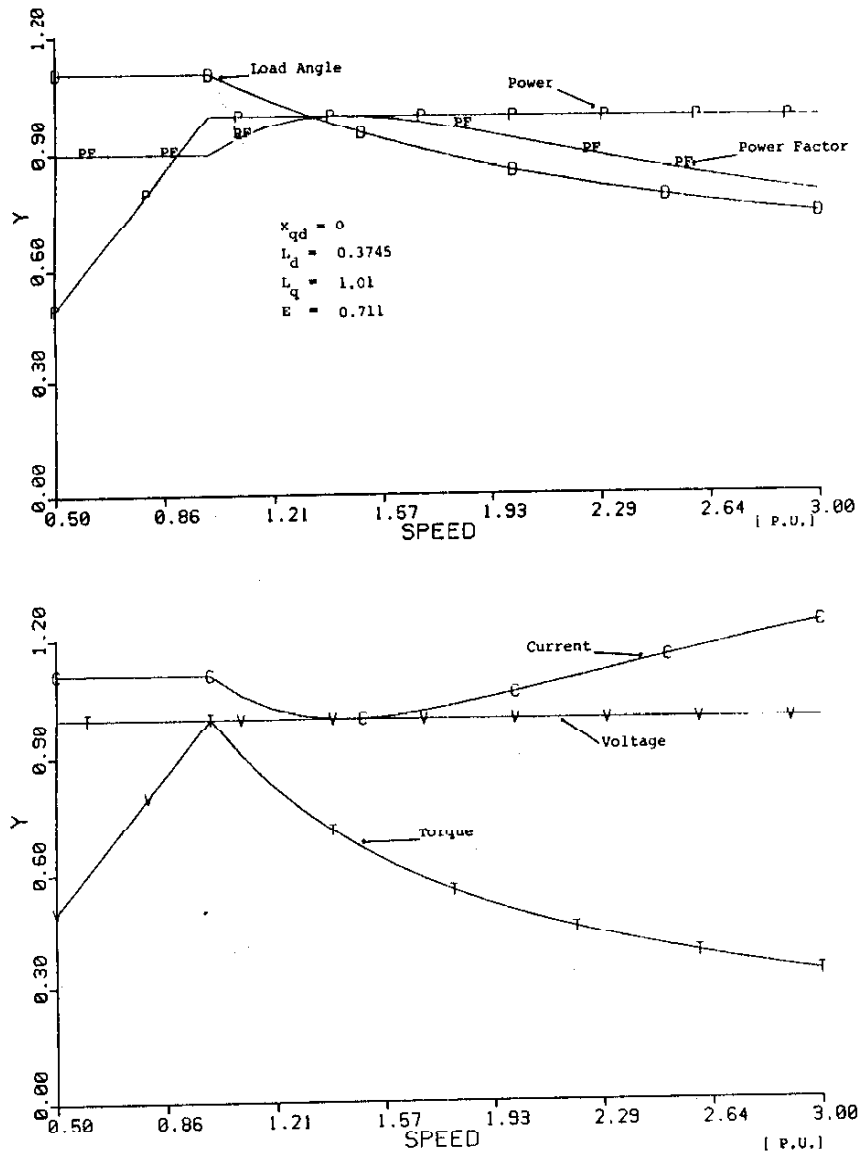


Fig. 11. Salient pole machine characteristics as function of speed. Machine without cross coupling, constant power operation.

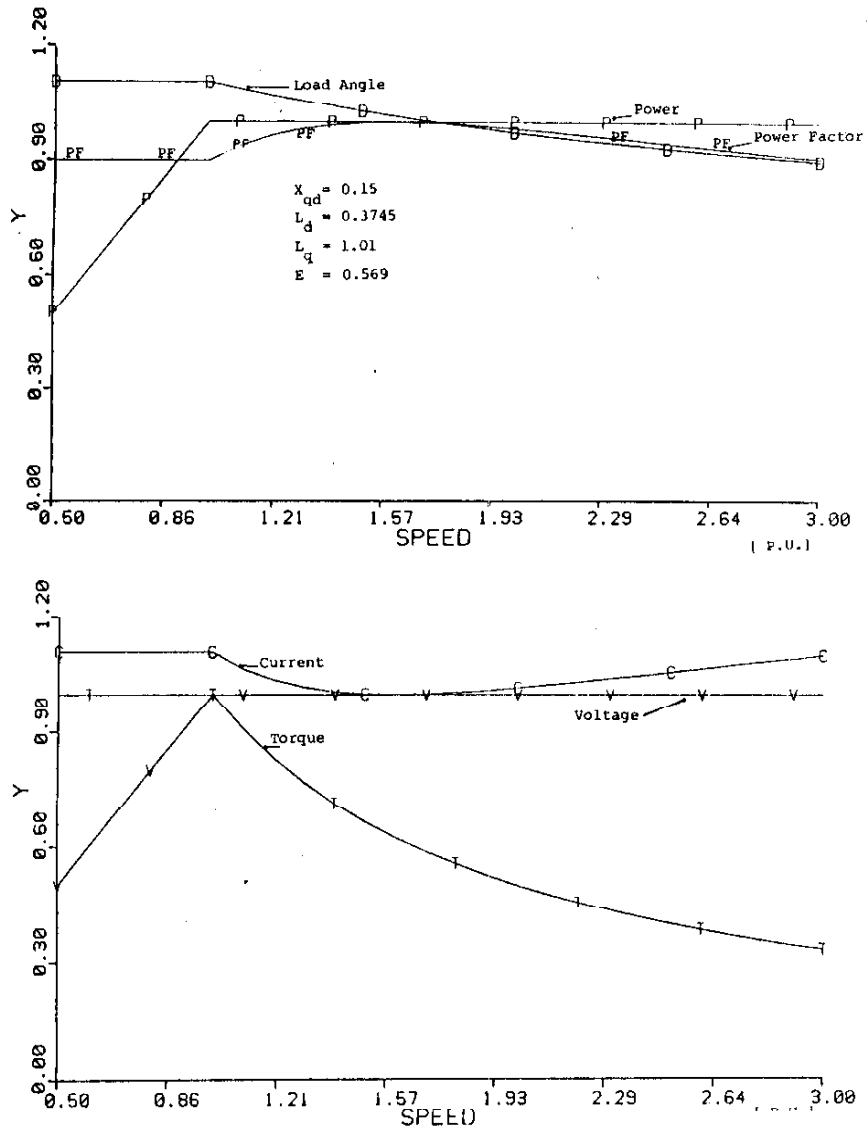


Fig. 12. Salient pole machine characteristics as function of speed. Machine with cross coupling, constant power operation.

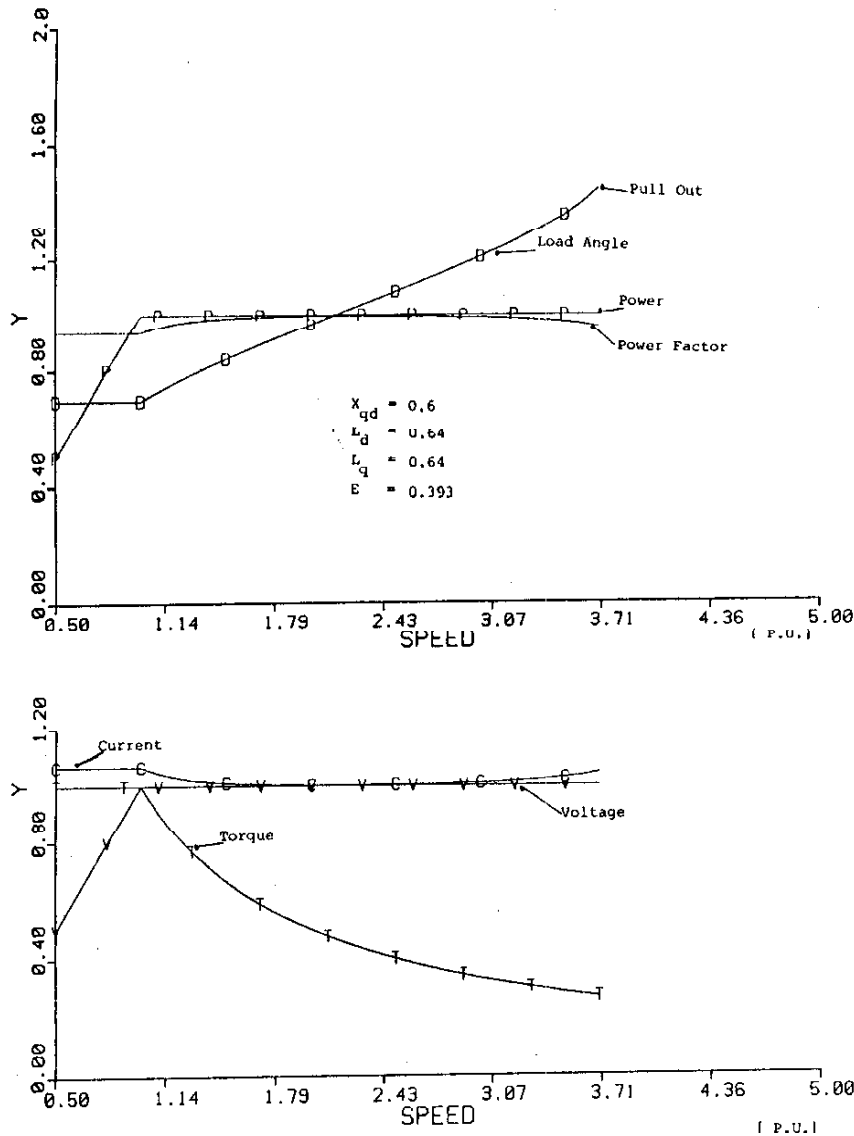


Fig. 13. Characteristics of machine with very large  $X_{qd}/X_q$  ratio.

observe that the machine with cross coupling delivers an almost constant power, for constant current, while the power delivered by the machine without cross coupling decreases rapidly. The useful speed range is in this case noticeably larger than expected from a permanent magnet machine. The same comparison is done in Figs. 11 and 12, but in this case the power is kept constant above base speed. Again, this cross coupling effect is seen to be advantageous with a much slower rise of the current as speed increases.

*Disadvantages of Cross Coupling*

It is important to note that the cross coupling effect is not always advantageous. As shown earlier, such coupling can cause higher currents at low torque and also shorten the overall useable speed range. Fig. 13 shows the computed characteristics of a hypothetical machine with very large  $X_{qd}/X_q$  ratio. Such a machine will behave fairly well with constant power until 4-pu speed, where pullout occurs. The same problem

occurs for machines with usual values of  $X_{qd}$  but at much higher speeds.

**INFLUENCE OF CROSS COUPLING AS VIEWED FROM THE AIR GAP VOLTAGE—ORIGIN OF THE PHENOMENON**

In order to understand the mechanism behind the cross coupling phenomenon, a full pitch search coil was placed in the stator slots of the machine described in the Appendix. The coil was used to provide a picture of the flux density along the air gap. Waveforms of the voltage at the terminals of the coil are shown in Fig. 14; trace A represents the waveform when the machine is driven as a generator on open circuit. Traces B and C show the waveforms when the machine is run with almost no  $q$  axis current or no  $d$  axis current, respectively. Trace A shows a square wave representing the flux due to the magnets only. The tilt in the waveform is apparently due to eddy currents and disappears at low speeds. Traces B and C



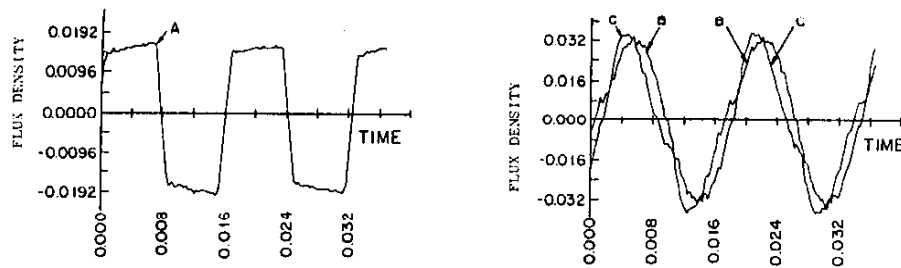


Fig. 14. Measured air gap voltage waveforms. Trace A: open circuit operation. Trace B: No  $q$  axis current. Trace C: no  $d$  axis current.

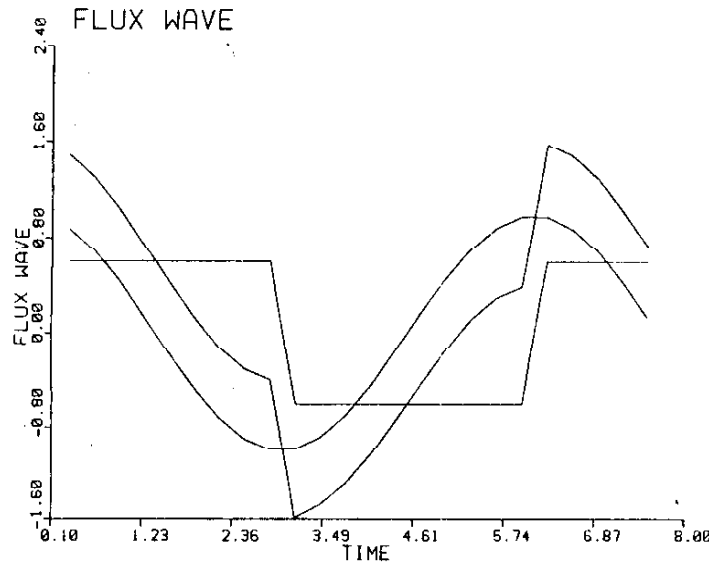


Fig. 15. How superposition of square wave and sine wave approximates results of Fig. 14, trace C.

show the additional influences of the sinusoidal stator MMF. These curves can be approached theoretically by the superposition of the square wave and a sine wave phase shifted by the proper angle. This theoretical result is shown in Fig. 15.

The influence of the cross coupling factor on the amplitude of the air-gap flux can be shown as follows. Knowing the values of the parameters  $X_d$ ,  $X_q$ , and  $X_{qd}$  and having measured  $I$ ,  $V$ ,  $\delta$ , and PF, it is possible to carry out the following calculations, using the values of the fundamental components.

#### Classical Model:

- a)  $X_d I_d = 0.809$   
 $V_q = E + X_d I_d = 2.090$   
 $X_q I_q = 0.8816$   
 $V = 3.04 \cos(\omega t - 16.8^\circ)$ .
- b)  $X_d I_d = 0.1037$   
 $V_q = E + X_d I_d = 2.2037$   
 $X_q I_q = 1.811$   
 $V = 2.85 \cos(\omega t - 39.4^\circ)$ .

#### New Model:

- a)  $X_d I_d = 0.809$   
 $X_{qd} I_q = 0.131$   
 $V_q = E + X_d I_d + X_{qd} I_q = 3.04$   
 $X_q I_q = 0.8816$   
 $V = 3.16 \cos(\omega t - 16.2^\circ)$ .

- b)  $X_d I_d = 0.1037$   
 $X_{qd} I_q = 0.269$   
 $V_q = E + X_d I_d + X_{qd} I_q = 2.472$   
 $X_q I_q = 1.811$   
 $V = 3.06 \cos(\omega t - 36^\circ)$ .

The numerical values shown are scaled values obtained from the measurements and are for purposes of comparison only. The applied voltage being the same in both cases (230 V line to line), the fundamentals of the two waveforms should be equal. In the case where  $X_{qd}$  is not used (classical model), it can be noted that a substantial difference exists between the values calculated in the two cases. This difference is significantly reduced when the complete model is used. The calculated results are consistent with the value provided by the measured waveforms.

It is reasonable to think of the cross coupling effects as a result of the redistribution of the flux in the air gap. This redistribution occurs because the magnets are buried in the rotor, behind a certain mass of iron which the flux has to cross before reaching the air gap. Saturation of the iron in this pole piece above the magnet is the cause of the redistribution of flux. As might be anticipated, the cross coupling factor varies with the flux density. Fig. 16 presents the measured variation as a function of the air gap voltage.

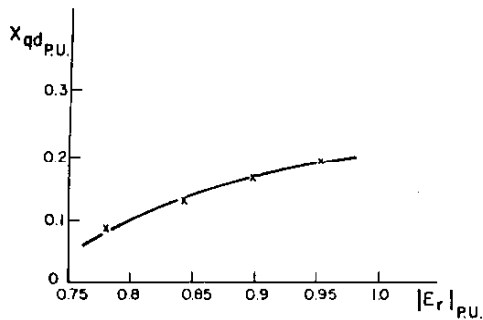


Fig. 16. Cross coupling factor as function of air gap voltage.

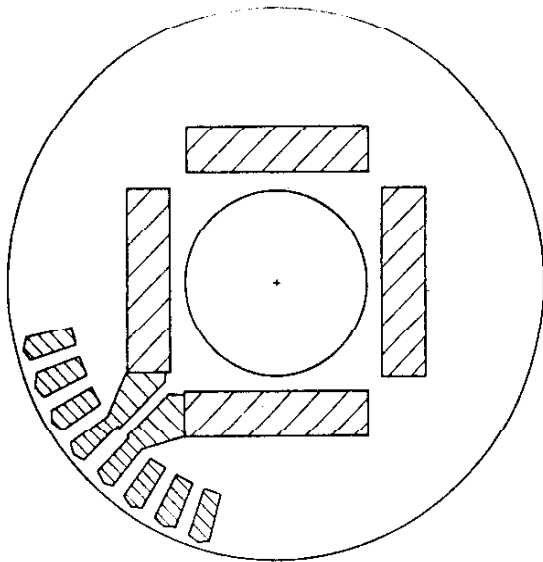


Fig. 17. Schematic of magnet arrangement in rotor of machine.

## CONCLUSION

A new machine model involving a cross coupling  $X_{qd}I_q$  voltage drop in the  $q$  axis is presented. This effect is shown to have an important field weakening action in the constant horsepower region. This term in the  $d - q$  model has been shown to be related to a redistribution of the rotor (magnet) flux, resulting from  $q$  axis saturation.

## APPENDIX

The test motor has the following nameplate data: Reliance Electric Company, 2 hp, 115/230 V, 10.6/5.13 A, 60 Hz, 1800 r/min. Fig. 17 shows a schematic of the magnet arrangement in the rotor of the machine.

## REFERENCES

- [1] B. Sneyers, G. Maggetto, and J. L. Van Eck, "Inverter fed permanent magnet synchronous motor for road electric traction," presented at the Int. Conf. on Electrical Machines, Budapest, Sept. 5-8, 1982.



Brigitte Sneyers was born in Brussels, Belgium, in 1956. She graduated as an Electrical Engineer from the Free University of Brussels in 1979 and studied at the University of Wisconsin, Madison, in 1982-1983.

She worked as a Research Assistant between 1979 and 1982 and again after her return from the University of Wisconsin. Her fields of interest include ac drives and power electronics.



Donald W. Novotny (M'62-SM'77) received the B.S. and M.S. degrees in electrical engineering from the Illinois Institute of Technology, Chicago, in 1956 and 1957 and the Ph.D. degree from the University of Wisconsin, Madison, in 1961.

Since 1961 he has been a member of the faculty at the University of Wisconsin Madison where he is currently Professor and Director of the Wisconsin Electric Machines and Power Electronics Consortium (WEMPEC). He served as Chairman of the Electrical and Computer Engineering Department from 1976 and 1980 and as an Associate Director of the University-Industry Research Program from 1972 to 1974 and from 1980 to the present. He has been active as a consultant to many organizations including Marathon Electric Company, Borg Warner Corporation, Barber Coleman Company, Otis Elevator Corporation, Allen Bradley Company, Eaton Corporation, and the Wisconsin Department of Natural Resources. He has also been Visiting Professor at Montana State University and the Technical University of Eindhoven, Eindhoven, Netherlands and a Fulbright Lecturer at the University of Ghent, Ghent, Belgium. His teaching and research interests include electric machines, variable frequency drive systems and power electric control of industrial systems.

Dr. Novotny is a member of ASEE, Sigma Xi, Eta Kappa Nu, and Tau Beta Pi and is a Registered Professional Engineer in Wisconsin.



Thomas A. Lipo (M'64-SM'71) received the B.E.E. and M.S.E.E. degrees from Marquette University, Milwaukee, WI, in 1962 and 1964, respectively, and the Ph.D. degree in electrical engineering from the University of Wisconsin in 1968. He was an NRC postdoctoral fellow at the University of Manchester Institute of Sciences and Technology, Manchester, England, during 1968-1969.

From 1969 to 1979 he was an Electrical Engineer in the Power Electronics Laboratory of Corporate Research and Development of the General Electric Company, Schenectady, NY. While at General Electric, he pioneered the computer simulation of many types of converter systems including cycloconverters, pulsewidth modulation voltage inverters, current-source ASCI inverters, third harmonic commutated CSI inverters, and load commutated converters. He was also heavily engaged in the development of algorithms for control of solid-state converter drives for which he received several IEEE Prize Paper Awards and has received five patents with two additional pending. He has published over 60 technical papers, contributing to the analysis and design of a wide range of industrial applications including ac drives for ball mills, pumped hydro, excavators, as well as traction drives for transit cars, locomotives, and off-highway vehicles. He is currently a Professor in the Department of Electrical and Computer Engineering, University of Wisconsin-Madison.

Dr. Lipo serves on the IAS Industrial Drives Committee, the IES Drives Committee and the PES Synchronous Machine Subcommittee, Electric Machine Theory Subcommittee, and Induction Machine Subcommittee of which he is a past Chairman. He has also served on the Program Committee for the IEEE Power Electronics Specialists Conference for the past six years and was Program Chairman in 1979. He is a member of the Steering Committee for the International Conference on Electrical Machines, an Associate Editor of the journal *Electric Machines and Power Systems* and Editor of the forthcoming *IEEE Journal of Power Electronics*. He is a member of Pi Mu Epsilon, Eta Kappa Nu, Tau Beta Pi, and Sigma Xi.